Calculation of total column ozone from global UV spectra at high latitudes

G. Bernhard and C. R. Booth

Biospherical Instruments Inc., San Diego, California, USA

R. D. McPeters

NASA Goddard Space Flight Center, Greenbelt, Maryland, USA

[1]   A new algorithm to retrieve total column ozone from global spectral UV irradiance measurements is presented, and its accuracy is assessed. The expanded uncertainty (coverage factor 2) of the resulting ozone values varies between 2% and 3.5% for solar zenith angles (SZA) smaller than $75°$ and clear skies. For larger SZA the uncertainty becomes dominated by the sensitivity of the method to the atmospheric ozone distribution. Using this algorithm, ozone values were calculated from UV spectra measured by the National Science Foundation's SUV-100 spectroradiometer at Barrow, Alaska, between 1996 and 2001. Special attention was given to March–April 2001, the period when the campaign "Total Ozone Measurements by Satellites, Sondes, and Spectrometers at Fairbanks" (TOMS³F) took place. The data set was compared with observations by NASA's Earth Probe Total Ozone Mapping Spectrometer (TOMS) and a Dobson spectrophotometer operated by NOAA's Climate Monitoring and Diagnostics Laboratory (CMDL) at Barrow. On average, the new algorithm generates ozone values in spring 2.2% lower than TOMS observations and 1.8% higher than Dobson measurements. From the uncertainty budget and the comparison with TOMS and Dobson it can be concluded that ozone values retrieved from global UV spectra have a similar accuracy as observations with standard instrumentation used for ozone monitoring. The new data set can therefore be used for validation of other ozone data.   *INDEX TERMS:* 0360 Atmospheric Composition and Structure: Transmission and scattering of radiation; 0394 Atmospheric Composition and Structure: Instruments and techniques; 3359 Meteorology and Atmospheric Dynamics: Radiative processes; *KEYWORDS:* total column ozone, ozone profile, ultraviolet radiation measurements

1.   Introduction

[2]   A new algorithm to calculate total column ozone from global irradiance measurements has recently been proposed [*Bernhard et al.*, 2002]. Here we present a thorough uncertainty evaluation of the method and a comparison of the resulting data set with TOMS and Dobson measurements at Barrow, Alaska. One objective of the investigation is to assess the accuracy of the method for high latitudes where prevailing SZAs are large. A second goal is to evaluate the feasibility of using global irradiance data for the validation of ozone values from standard instrumentation. One advantage compared to TOMS and Dobson observations is that ozone values from global UV spectra can be provided at high frequency (in our case one value every 15 min), regardless of weather conditions.

[3]   This research was motivated by the campaign "Total Ozone Measurements by Satellites, Sondes and Spec-trometers at Fairbanks" (TOMS³F), which took place between mid-March and end of April 2001. This undertaking involved the comparison of ozone measurements from various instruments with the goal to help reveal and explain systematic errors in the different data sets. Location and time of the campaign were chosen based on the fact that the largest discrepancies between TOMS and Northern Hemisphere ground-based stations occur when ozone values are high (e.g., 500 DU) and SZAs are large [*McPeters and Labow*, 1996]. These conditions lead to low radiation levels at short wavelengths, and subsequent systematic errors in ground-based measurements related to detection limit and stray light problems. Satellite ozone retrievals are also affected, because satellites do not "see" to the ground under these conditions, and errors may occur when ozone is added to the reported total column value to account for the contribution from the lower troposphere.

[4]   The idea of calculating total ozone from spectra of global irradiance was first proposed by *Stamnes et al.* [1991]. Their method calculated ozone from the ratio of spectral irradiance at 305 and 340 nm. A model is used to

calculate a synthetic chart of this ratio as a function of column ozone amounts and solar zenith angle. The column ozone amount is then derived by matching the observed irradiance ratio on any particular day to the appropriate curve of the chart.

[5] In contrast to the method of *Stamnes et al.* [1991], the method presented here requires several model runs for every irradiance spectrum. Although more elaborate, the advantage is that atmospheric parameters (e.g., albedo, ozone and temperature profiles) can be optimized for each spectrum without having to process a new chart for each set of conditions. This will lead to reduced uncertainties, in particular at large SZAs. However, our method is also applicable when only climatological data is available and will generally lead to ozone values of good accuracy, except for times when the SZA is larger than 75°. Above 75°, knowledge of the ozone profile becomes essential. A wavelength interval for the short-wavelength band is used in our retrieval algorithm, which is automatically adjusted depending on irradiance levels. This reduces uncertainties related to the instrument's detection limit that may affect more commonly used algorithms that are based on fixed wavelengths for ozone determination. Furthermore, our method produces a spectrum of the measurement/model ratio for every measurement, allowing one to assess the quality of the results and to filter for outliers.

2. Instrumentation and Data

[6] Global (Sun+sky) spectral irradiance measurements were performed by a SUV-100 spectroradiometer (Biospherical Instruments Inc.) at Barrow, Alaska (71°18′N, 156°47′W, 10 m above sea level). The instrument is part of the National Science Foundation's Office of Polar Programs (NSF/OPP) UV monitoring network. Details of the instrument and data processing were published by *Booth et al.* [1994, 2001, and references therein]. Measurements in the wavelength range 280–605 nm are performed quarter-hourly. The instrument has a spectral resolution of 1.0 nm. The time required for one spectral measurement is 10.5 min (2.0 min between 305 and 335 nm). All results presented here are based on "Level 3" data [*Booth et al.*, 2001], available on the Internet www.biospherical.com/NSF. Data cover the period July 1996–June 2001. Data from 1996 and 1997 were postcorrected to improve their wavelength accuracy (see Uncertainty Section). Published solar UV data from the NSF network are currently not corrected for the effect of the fore-optic's cosine error. For this study, data were corrected based on the method described by *Seckmeyer and Bernhard* [1993].

[7] Values of total column ozone calculated from SUV-100 measurements were compared with Earth Probe TOMS overpass data for Barrow and ground-based Dobson spectrophotometer observations performed by NOAA/CMDL at their facility at Barrow. Since mid-2000, the TOMS instrument has experienced a wavelength-dependent loss in sensitivity due to degradation of the front scan mirror, which causes a scan angle dependent variation in the instrument's throughput. This problem introduces a latitude, SZA, and total ozone dependent error of several DU into the TOMS data, which is partly corrected by the TOMS team. Figure 1 shows the ratio of corrected/uncorrected data. The
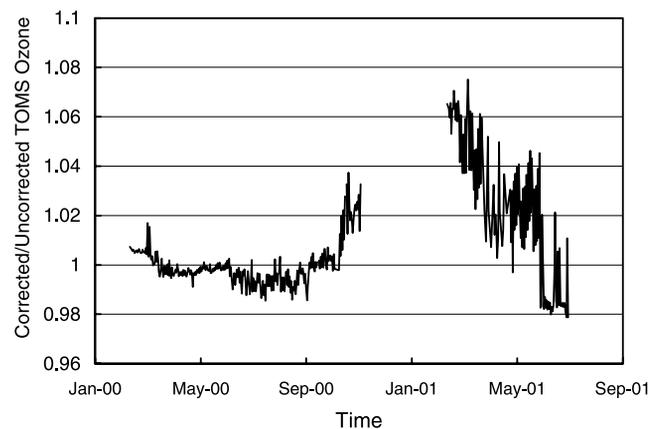

Figure 1. Ratio of corrected/uncorrected Earth Probe TOMS data at Barrow.

corrected data set is higher by 2–6% between February and May 2001. For October 2000 and June 2001, corrections are smaller than 3%. Both the corrected and uncorrected data set were compared with SUV-100 data.

[8] All available CMDL Dobson measurements were used, including "direct Sun" and zenith observations for Dobson "AD" as well as "CD" pairs. Ozone values based on "direct Sun" observations showed a somewhat lower scatter than zenith sky observations during cloudy conditions, as can be expected, but there is no significant bias between the two data sets, which would have warranted a separate analysis.

[9] Several data sets of ozone and temperature profiles were used:

[10] 1. Standard profiles for "subarctic summer" (denoted in the following as "AFGLSS") and "subarctic winter" ("AFGLSW") conditions, provided by the Air Force Geophysics Laboratory [*Anderson et al.*, 1986].

[11] 2. Profiles measured by CMDL with balloon sondes at Fairbanks, Alaska (64°51′N, 147°50′W) in 1997 (April–November) and 2001 (March and April). Data were obtained from ftp.cmdl.noaa.gov/pub/ozone/. The profiles were extrapolated to include values above the balloon's burst altitude, utilizing an algorithm described by *Bernhard et al.* [2002]. The data set is denoted "CMDL." Total column ozone values calculated from these profiles agreed to within a few Dobson Units with total ozone values stated in the CMDL data files. The latter are based on an extrapolation method described by *McPeters et al.* [1997], which utilizes a climatology of ozone profiles measured by Nimbus 7 solar backscattered ultraviolet (SBUV) instrument. Based on altitude, pressure and temperature information given in the CMDL data set, the air density profile was also adjusted. For ozone retrievals during the March–April 2001 period, profiles measured closest in time with the SUV-100 measurements were selected.

[12] 3. Ozone profiles measured by the NOAA 16 SBUV/2 satellite during March and April 2001. Profiles are given as ozone mixing ratios for 17 standard pressure levels between 0.5 and 100 mbar, and in layer ozone amounts as a function of Umkehr pressure levels. For use in the ozone retrieval algorithm, the profiles were converted to ozone concentration (in molecules per cm^3) as a function of altitude. For this

conversion, altitude, pressure, and temperature profiles are required, which are not part of the NOAA 16 SBUV/2 data set. These profiles were taken from either the AFGLSS or AFGLSW profile, and the resulting ozone profiles are consequently denoted "NOAA16SS" and "NOAA16SW". Total column ozone values calculated from the converted profiles typically agree to within 4 DU (<1% difference) with the column value explicitly stated in the NOAA 16 SBUV/2 data, giving confidence in the conversion process. Altitude, pressure, temperature, and air density profiles used with both NOAA 16 profiles are identical to the profiles of AFGLSS and AFGLSW, respectively. Only profiles measured within a range of ±1° latitude and ±10° longitude of Barrow were used. With this restriction, there is still at least one profile per day.

[13] 4. NOAA 11 SBUV/2 ozone profiles, measured between 1989 and 1994. The profiles were converted in a similar fashion as the NOAA 16 SBUV/2 profiles and are denoted "SBUV2SS" and "SBUV2SW". Profiles from all years were averaged over 14-day periods (i.e., 1-March–15-March, 16-March–31-March, 1-April–15-April, etc.) to provide climatological mean profiles for Barrow.

3. Ozone Retrieval Algorithm

[14] The new algorithm for retrieving total column ozone values from global irradiance spectra is based on the comparison of measured spectra from the SUV-100 instrument with results of the radiative transfer model UVSPEC/libRadtran available at www.libradtran.org [*Mayer et al.*, 1998]. The model's pseudospherical radiative transfer solver with twelve streams is used. The *Bass and Paur* [1985] ozone absorption cross section was implemented throughout the paper, as this is the cross section that is also used in the Dobson and TOMS algorithms. Its temperature dependence was parameterized with a second-degree polynomial. Aerosol optical depths were parameterized with the Ångstroem turbidity formula. The Ångstroem parameters alpha and beta were set to 1.3 and 0.046, respectively. The extraterrestrial spectrum up to a wavelength of 407.75 nm was measured by the Solar Ultraviolet Spectral Irradiance Monitor (SUSIM) onboard the space shuttle during the ATLAS-3 mission. An annual cycle in albedo was specified with albedo = 0.05 in summer and 0.85 in winter (see Uncertainty Section). Ground pressure was set to 1015 hPa. The model did not consider clouds. It is shown below that the clear-sky model can also be applied to cloudy days, resulting in only small uncertainties in the retrieved ozone values. The change in SZA during the course of a scan was taken into account in all model calculations.

[15] Several model runs with different values of the model input parameter "ozone column" were performed for every measured spectrum. The deviation between measurement and model is determined dependent upon the ozone value used by the model. This deviation is quantified with the ratio R:

$$R = \frac{\frac{1}{n}\sum_{\lambda=\lambda_S}^{315\text{nm}} Q(\lambda)}{\frac{1}{m}\sum_{\lambda=325\text{nm}}^{335\text{nm}} Q(\lambda)}, \qquad (1)$$
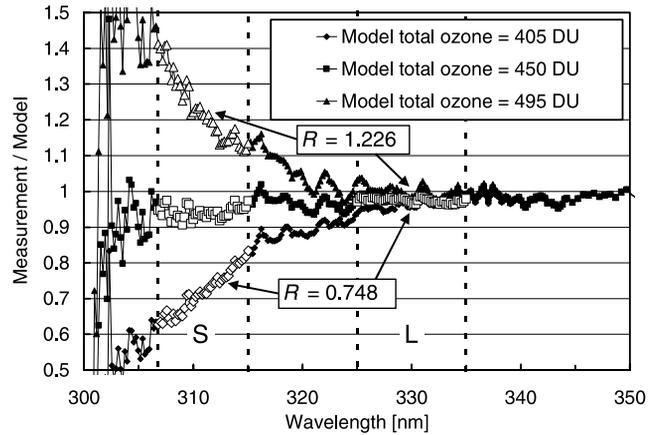

Figure 2. Ratios of measurement and model for model ozone values of 405 DU (diamonds), 450 DU (squares), and 495 DU (triangles). The ratios are based on a spectrum that was measured on 4/1/01 at 19:45 UT. Vertical lines indicate the limits of the short-wavelength interval (306.8–315 nm; symbol "S") and long-wavelength interval (325–335 nm; symbol "L") that were used for the ozone retrieval. Ratios within these intervals are indicated by large symbols. R-ratios are given for the calculations with 405 DU ($R = 0.748$) and 495 DU ($R = 1.226$).

where $Q(\lambda)$ is the ratio of measured to modeled global spectral irradiance at wavelength λ. The numerator of R is the average of the ratios $Q(\lambda)$ for wavelengths strongly affected by ozone absorption. The denominator of R is the average of the ratios $Q(\lambda)$ in the spectral band 325–335 nm, which is only weakly affected by ozone absorption. The number of addends, n and m, is determined by the number of discrete measurements of spectral irradiance $R(\lambda)$ by the SUV-100. By using the average of $Q(\lambda)$ over a several nm wide wavelength band rather than the measurement at a single wavelength, uncertainties due to wavelength shifts, bandwidth effects, noise, and uncertainties introduced by the Fraunhofer lines in the solar spectrum and the fine structure in the ozone absorption cross section can be reduced. The wavelength λ_S is chosen such that measured irradiance $E(\lambda)$ at wavelengths $\lambda > \lambda_S$ is larger than 1 mW/(m² nm). By making the lower wavelength limit dependent on the measured spectrum, measurements near the instrument's detection limit do not contribute to the average, and profile related uncertainties are reduced as well (see below). The total ozone value resulting from this method is the model ozone value that leads to $R = 1$.

[16] The algorithm is illustrated in Figure 2, which shows ratios of a measured spectrum to three associated model spectra that were calculated for ozone values of 405, 450 and 495 DU. The agreement is best for the calculation with 450 DU ($R = 0.957$). For 405 DU, the R-ratio is 0.748; for 495 DU, it is 1.223. Model ozone value is typically varied within a range of ±20% either around an ozone value from another source, or a climatological value. The ozone value retrieved by the algorithm depends little on the initial value, and any dependency is reduced to negligible amounts (i.e., <0.5 DU) by calculating the set of model spectra in sufficiently small ozone steps. For comparison with TOMS
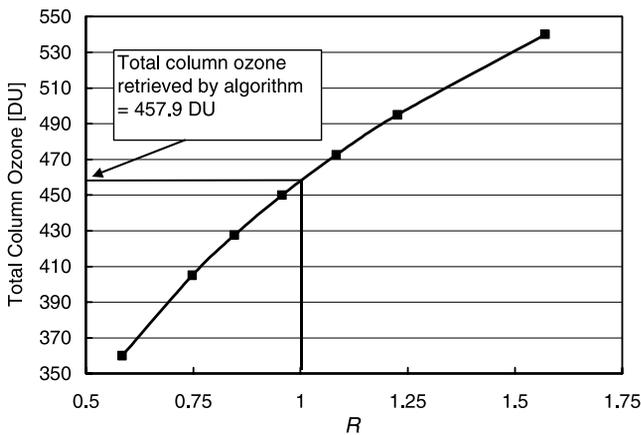
Figure 3. Relationship of ozone value used in the model and R-ratio. The ozone value returned by the algorithm is the ozone value that leads to $R = 1$.

Figure 4. Ratios of ozone values calculated with the CMDL, NOAA16SS, and NOAA16SW profiles measured in March and April 2001. The results of the CMDL profiles were scaled with equation (2) to reduce temperature effects.

or Dobson observations, seven different model ozone values were used, which were set to 0%, ±5%, ±10%, ±20% of the respective TOMS or Dobson value.

[17] Figure 3 shows the relationship between the R-ratio and the ozone value used in the model for the example spectrum depicted in Figure 2. The relationship is a smooth function. The ozone value leading to $R = 1$ is therefore well defined, and was found to be 457.9 DU for the spectrum chosen.

4. Uncertainty of Ozone Retrieval Algorithm

[18] All uncertainties were estimated in accordance with the *International Standards Organization* (*ISO*) [1993]. As the retrieval algorithm is based on a comparison of measured and modeled spectra, all parameters that spectrally change the model result will also affect the calculated ozone values. The resulting uncertainty in ozone was determined by varying all relevant model parameters over reasonable limits, and quanti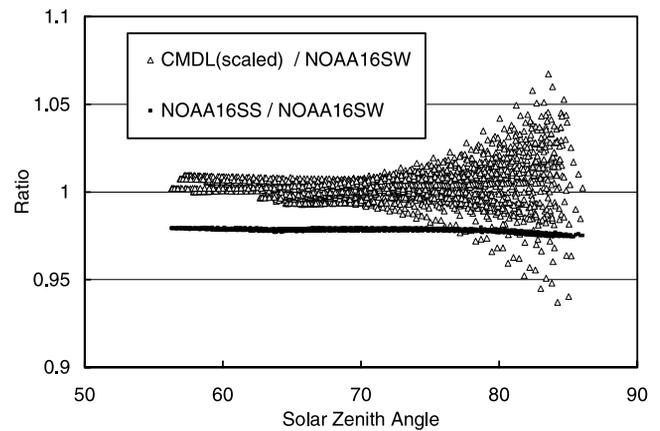fying the effect on the ozone output. The complete uncertainty budget is compiled in Table 1 and further explained in the following.

4.1. Ozone Profile

[19] Uncertainties related to the vertical distribution of ozone have the same physical causes as the Umkehr effect [*Götz*, 1931]. For their quantification, all spectra measured between March 15 and April 30, 2001 were processed with the CMDL, AFGLSW, NOAA16SW, NOAA16SS, and SBUV2SW profiles, and the ozone values resulting from the different data sets were ratioed against the ozone values derived with the NOAA16SW profiles. The results are depicted in Figures 4 and 5. We chose the NOAA16SW profiles as the reference as evidence given below suggests that this set of profiles represents best the actual conditions at Barrow during the time of the TOMS[3]F campaign.

[20] The ratio of ozone values calculated with the CMDL and NOAA16SW profiles agree to within ±1% for SZA smaller than 70° (Figure 4). For larger SZAs, the scatter gradually increases to reach ±7% at SZA = 85°. In general,

Table 1. Uncertainty Overview[a]

Error Source	Standard Uncertainty, %							
	March	April	May	June	July	Aug.	Sept.	Oct.
Systematic Errors								
Ozone profile, SZA < 75°		0.5(1.2)	0.5(1.2)	0.5(1.2)	0.5(1.2)	0.5(1.2)	0.5(1.2)	
Ozone profile, SZA = 80°	1.6(2.1)							1.6(2.1)
Temperature profile, variability	0.48	0.84	0.05	0.09	0.09	0.26	0.38	0.36
Temperature profile, offset	0.11	0.11	0.05	0.05	0.05	0.05	0.05	0.05
Clouds, spectral effect	0.11	0.20	0.38	0.45	0.63	0.96	0.84	1.23
Albedo	0.17	0.17	0.43	0.48	0.02	0.02	0.02	0.48
Aerosols	0.22	0.22	0.22	0.22	0.22	0.22	0.22	0.22
Ground pressure	0.10	0.10	0.10	0.10	0.10	0.10	0.10	0.10
Wavelength shift	0.54	0.54	0.54	0.54	0.54	0.54	0.54	0.54
Absolute calibration	0.33	0.33	0.33	0.33	0.33	0.33	0.33	0.33
Combined uncertainty	1.8(2.3)	1.2(1.6)	1.0(1.5)	1.1(1.5)	1.1(1.5)	1.3(1.7)	1.3(1.7)	2.2(2.6)
Expanded uncertainty ($k = 2$)	3.6(4.5)	2.4(3.3)	2.0(3.0)	2.1(3.1)	2.1(3.0)	2.6(3.4)	2.5(3.3)	4.4(5.2)
Random Errors								
Clouds, time effect	1.00	1.00	1.88	2.50	2.50	2.50	2.50	2.50

[a]Values in parentheses are based on ozone calculations performed with climatological profiles rather than profiles measured close in time and space with UV spectra. Combined and expanded uncertainties take into account all systematic errors, but no random errors.
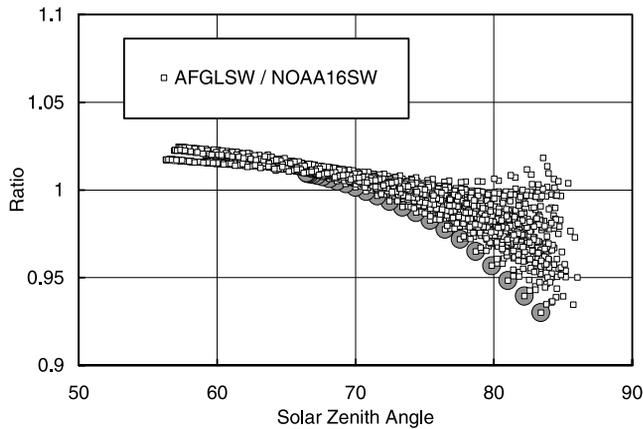
Figure 5. Ratios of ozone values calculated with the AFGLSW and NOAA16SW profiles. Data from April 1, 2001 are marked with circles.

there is little bias between the two data sets. NOAA16SW profiles are available for every day and were measured within ±1° latitude of Barrow. CMDL profiles on the other hand were measured in Fairbanks, which is about 6° latitude south of Barrow, and are not available for every day. The variation of the atmospheric ozone distribution over time and space may therefore explain the random variation between both data sets at large SZA.

[21] Ozone values calculated with AFGLSW profile are systematically higher than NOAA16SW-based results for SZA < 70° and smaller for SZA > 70° (Figure 5). In contrast to the CMDL and NOAA16SW profiles, the AFGLSW profile is a climatological mean profile, which is applicable to high latitudes of both hemispheres. The bias seen in Figure 5 suggests that this profile is systematically different from profiles prevailing at Barrow. In an attempt to explain the reasons for the SZA dependence, we analyzed data from April 1, 2001, in more detail (data marked with circles in Figure 5), and will discuss this below.

[22] Figure 6 contrasts four profiles: the NOAA16SW profile from April 1, 2001 (measured close to Barrow at
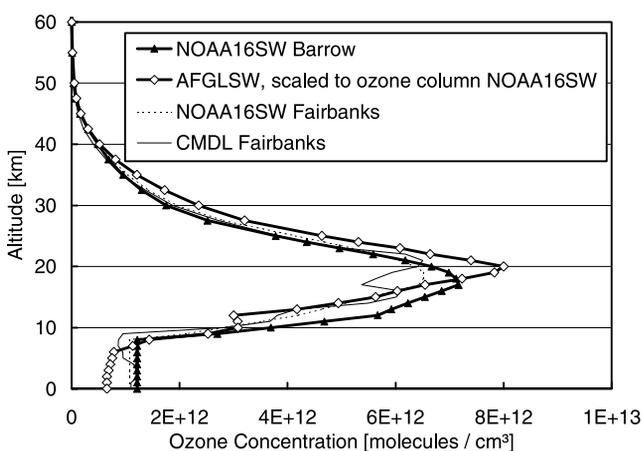

Figure 6. NOAA16SW profiles for Barrow and Fairbanks measured on April 1, 2001 in comparison with the CMDL profile measured at Fairbanks on the same day, and the AFGLSW profile.
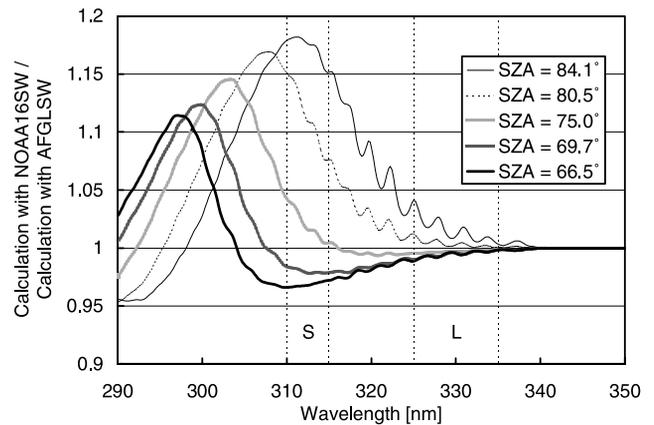

Figure 7. Ratios of UV spectra modeled with the NOAA16SW profile measured near Barrow on 4/1/02, and the AFGLSW profile for several SZAs. The vertical lines indicate the typical limits of the short-wavelength interval (310–315 nm; symbol "S") and long-wavelength interval (325–335 nm; symbol "L") used in the ozone retrieval algorithm.

71.98°N and 159.95°W; ozone column = 480 DU); the AFGLSW profile (scaled with a factor of 1.27 to gain the same ozone column as NOAA16SW); the NOAA16SW profile for Fairbanks (448 DU); and the CMDL EEC balloon sonde profile measured at Fairbanks on April 1, 2001 (428 DU). Both Fairbanks profiles agree well (except at heights around 17 km where the CMDL profile is 20% lower), confirming that balloon and satellite measurements are reasonably consistent. The Barrow profile is significantly higher, suggesting a real difference in the ozone distribution between the two sites for the given day. The scaled AFGLSW profile is significantly lower than the NOAA16SW profile in the troposphere and lower stratosphere, but higher at altitudes above 18 km. For small SZA, ozone at low altitudes is more effective in attenuating global UV radiation than ozone at higher altitudes, as photons are scattered more frequently by air molecules at lower atmospheric levels, leading to an amplification of tropospheric ozone absorption. For large SZAs, the effect is reversed, as photons from the direct solar beam are mostly absorbed before they reach the ground, and more and more photons travel through higher atmospheric layers before they are scattered toward the Earth's surface.

[23] The disproportionate role of tropospheric ozone was first described by *Brühl and Crutzen* [1989], and is illustrated in Figure 7 for the situation of April 1, 2001. Here, ratios of UV spectra modeled with the NOAA16SW Barrow profile and the AFGLSW profile are shown for various SZAs. For SZAs < 75°, spectra calculated with the NOAA16SW profile are lower in the 310–315 nm wavelength band than spectra based on AFGLSW: as ozone concentrations of the NOAA16SW profile are more weighted toward the troposphere, the profile is more effective in absorbing UV radiation than AFGLSW. The ozone retrieval algorithm compensates the higher absorption effectiveness with a smaller total ozone output. For SZAs > 75°, the effect is reversed, in agreement with theory. At 315 nm, there is a

15% difference for the spectra measured at SZA = 84.1° (solid thin line in Figure 7).

[24] Figure 7 suggests that ozone profile related uncertainties could be reduced if the short wavelength band of the retrieval algorithm were moved to longer wavelengths for large SZAs. However, runs with a modified algorithm show that only a small improvement can be achieved. Because of the small irradiances at large SZA, the lower wavelengths λ_S for the short-wavelength average in equation (1) is already as high as 312.2 nm for the spectrum at SZA = 84.1. Calculations where the interval of the numerator of equation (1) was changed from 312.2–315 nm to either 318–319 nm or 317–320 nm decreased the sensitivity of the profile slightly, but lead to problems related to the (temperature dependent) fine structure of the ozone cross section, which becomes significant above 314 nm [Bass and Paur, 1985]. In addition, the smaller difference of numerator and denominator of equation (1) resulting from changing the short-wavelength interval to larger wavelengths makes the algorithm more susceptible to the influence of parameters other than ozone. We therefore conclude that the sensitivity to the ozone profile at large SZA is a principle limitation for the accuracy of ozone values calculated from global irradiance measurements at large SZA.

[25] The uncertainties related to ozone profile are given in Table 1 and are estimated from the variation of the different data sets shown in Figures 4 and 5. Two cases were considered: (i) When actual profiles are available, measured in close temporal and spatial proximity with the UV spectroradiometer; and (ii) when only mean climatological profiles are available. In the case of actual profiles, the uncertainty was estimated from the CMDL/NOAA16SW ratio. For average climatological profiles, the uncertainty was estimated from the AFGL/NOAA16SW and SBUV2SW/NOAA16SW ratios.

[26] From Figure 4 alone it is not possible to decide which set of profiles, either NOAA16SW or the CMDL, is more appropriate to be implemented for the comparison with TOMS and Dobson measurements. The NOAA16 profiles are measured more closely in time to the UV spectra, but they are more uncertain than the CMDL profiles at altitudes below 18 km. To address this problem, consider that at high latitudes hourly variations in ozone column are mainly caused by atmospheric dynamics rather than photochemistry. The change in total ozone occurring within one hour, ΔO_3, should therefore be independent of SZA. If ΔO_3 calculated from SUV measurements shows a significant, daily recurring SZA-dependence, the likely cause of this pattern is the use of an inadequate set of ozone profiles for the calculation rather than real changes in total ozone. For the quantification of this SZA dependence, we calculated the difference $\Delta O_3(t) = O_3(t + 1 \text{ hour}) - O_3(t)$ for four different ozone data sets. In addition to the two data sets that are based on the NOAA16SW and CMDL profiles, we also considered the AFGLSW data set and a forth data set based on semimonthly mean profiles. These mean profiles were constructed by averaging the daily NOAA16SW profiles over the 2-week periods March 15–31, April 1–15, and April 16–30 of 2001 ("NOAA16SW-2week"). In the last step, we calculated the standard deviation $\sigma(\Delta O_3(t))$ from all ozone data sets, separately for times when SZA is smaller than 75° and larger than 80°.

Table 2. Standard Deviation $\sigma(\Delta O_3)$ of Ozone Values Measured With a Time Difference of 1 Hour

	$\sigma(\Delta O_3)$ for	
Profile	SZA < 75°, %	SZA > 80°, %
NOAA16SW	1.23	1.58
NOAA16SW-2week	1.22	1.85
CMDL	1.25	1.94
AFGLSW	1.33	2.76

[27] Our results show that $\sigma(\Delta O_3(t))$ is smallest in both SZA-ranges when ozone data were calculated with the "daily" NOAA16SW profiles (Table 2). The standard deviations calculated with "NOAA16SW-2week" were significantly larger in the SZA > 80° segment, indicating that less accurate results are achieved when the daily variations in the ozone profile are not taken into account. The data set based on the CMDL profiles has a even larger standard deviation for the SZA > 80° segment, suggesting that the advantage of the profiles' higher vertical resolution cannot make up for the disadvantage of their larger spatial separation from Barrow. Based on these considerations, we used the "daily" NOAA16SW profiles for the comparison with TOMS and Dobson measurements (see Results Section).

4.2. Temperature Profile

[28] The ratio NOAA16SS/NOAA16SW is about 0.978, and varies only little with SZA (black squares in Figure 4). As mentioned before, both data sets are based on the same ozone profiles, but use the AFGLSS and AFGLSW temperature profile, respectively. The ozone-weighted average of the NOAA16SS temperature profile is 232.2 K; that of the NOAA16SW temperature profile is 218.4 K. In order to show that the factor of 0.978 is caused by the temperature dependence of the ozone absorption cross section (O_3CS), we calculated O_3CS as a function of wavelength for both mean temperatures. Between 305 and 315 nm (the wavelength interval relevant for the numerator of equation (1)), the temperature dependence of O_3CS is nearly constant with wavelength, and is on average a factor of 0.979 lower at 232.2 K than at 218.4 K. This factor is in excellent agreement with the ratio NOAA16SS/NOAA16SW shown in Figure 4, and it is therefore possible to parameterize the temperature dependence of the retrieved ozone value $O_3(T)$ in the same way as O_3CS:

$$O_3(T) = O_3(218.4\text{K})$$
$$*6.55/[7.36 + 0.021086 * (T - 273.13) + 0.00011484$$
$$*(T - 273.13)^2]. \qquad (2)$$

The coefficients used in equation (2) are the Bass and Paur O_3CS coefficients at 311.95 nm, which are representative for the 305–315 nm interval.

[29] To estimate the uncertainty related to the temperature profile, the ozone-weighted mean temperature was calculated from all CMDL profiles in a given month and translated into a standard uncertainty using equation (2). An additional uncertainty term related to stratospheric temperature variation was introduced, which takes into

Table 3. Effect of Clouds With High Optical Depth on Ozone Calculations

Source	Time, UT	Meas/Mod[a]	COD[b]	Cloud Extension, km	Droplet Size, μm	Ozone Profile	Calculated Ozone, DU	Difference to TOMS, %
TOMS	19:10						298.4	0.0
SUV	19:30	0.631	0.0			SBUV2[c]	296.6	−0.6
SUV	19:30	1.002	8.4	2−5	10	SBUV2[c]	300.5	0.7
SUV	22:45	0.167	0.0			SBUV2[c]	318.4	6.7
SUV	22:45	0.996	78.5	2−5	10	SBUV2[c]	309.73	3.8
SUV	22:45	0.998	78.5	3−8	10	SBUV2[c]	301.2	0.9
SUV	22:45	0.999	78.5	2−8	10	SBUV2[c]	297.2	−0.4
SUV	22:45	0.997	78.5	5−10	10	SBUV2[c]	294.7	−1.2
SUV	22:45	1.000	78.5	2−10	10	SBUV2[c]	285.8	−4.2
SUV	22:45	1.001	78.5	2−8	10	AFGLSS	284.3	−4.7
SUV	22:45	1.003	78.5	2−8	10	FB030[d]	280	−6.2
SUV	22:45	1.003	78.5	2−10	10	FB030[d]	271.5	−9.0
SUV	22:45	0.994	70.0	2−10	4	FB030[d]	273.1	−8.5

[a]Ratio of measurements and model at 340 nm.
[b]Cloud optical depth used in model calculations.
[c]NOAA 11 SBUV/2 average profile for 1−15 August.
[d]CMDL profile measured at Fairbanks on 4 July 1997.

account that the CMDL profiles were measured at Fairbanks rather than Barrow. The standard uncertainty was estimated from the difference of the subarctic and midlatitude AFGL temperature profiles.

4.3. Clouds

[30] Two factors primarily control uncertainties due to clouds. First, clouds lead to a wavelength-dependent attenuation of radiation, even though scattering from cloud droplets is almost wavelength independent in the UV. This dependence is partly caused by enhancement of the photon path due to multiple scattering in the cloud, which leads to an amplification of absorption by tropospheric ozone [*Mayer et al.*, 1998]. We quantified uncertainties related to this effect by comparing ozone values calculated with the standard procedure with results of a modified procedure, where the model input included a stratiform cloud, located between either 2−4 km or 2−8 km altitude. The cloud optical depth was chosen such that the difference between measured and modeled spectra became minimal at 340 nm. For a cloud of optical depth of 15, ozone values calculated with the clear-sky model were between 1% (cloud between 2 and 4 km) and 2% (cloud between 2 and 8 km) larger than the cloud model. These results are in good agreement with similar estimates by *Stamnes et al.* [1991] and *Masserot et al.* [2002].

[31] A cloud with optical depth of 15 leads to a reduction of erythemal irradiance by approximately 50%. By comparing values of erythemal UV measured in 1999 with results of the clear sky model, we calculated that cloud cover at Barrow reduces erythemal UV irradiance on the average by about 15% in May and June, 25% in July, and 40% during August through October. Only 0.4% of all spectra with SZAs smaller than 75° measured in 1999 exceeded 83% attenuation by clouds. The maximum reduction was 90%, which corresponds to a cloud optical depth of about 150. Systematic errors by the retrieval algorithm from thick clouds are difficult to estimate because they depend on the altitude extension of clouds and ozone concentration within the cloud. Both quantities are not known with sufficient accuracy. Estimates based on several sample spectra indicate that errors are likely smaller than 10% for

Barrow. As an example, we present ozone values calculated for a spectrum that was measured on August 12, 1999, at 22:45 UT. The SZA was 57° and the cloud optical depth (COD) at 340 nm was estimated to be 78.5. Measurements with an independent broadband sensor performed during this scan indicated that radiation levels were constant to within ±0.1% during the period when the SUV-100 spectroradiometer was scanning between 305 and 335 nm.

[32] The TOMS ozone value for 8/12/99 is 298.4 DU. (TOMS of course does not measure ozone below cloud level but adds a climatological amount to account for below cloud ozone.) The SUV-100 ozone value calculated for this day with the standard method for a time when the cloud influence was comparatively small (COD = 8.4) was 296.6 DU. Ozone values for the scan at 22:45 UT varied between 318 DU (clear sky model) and 270 DU (model with cloud between 2−10 km, CMDL profile), see Table 3. Ozone values calculated with the clear sky model are highest, in agreement with theory, as increased scattering within the cloud leads to more effective absorption by ozone molecules within the cloud, which is interpreted by the algorithm as a higher ozone column. Calculations with the cloud between 2 and 8 km, and the SBUV2SS ozone profile for 1−15 August resulted in an ozone value of 297 DU, demonstrating that a reasonable choice of cloud height and ozone profile will lead to an ozone value that is in close agreement with TOMS. The results further suggest that an overestimation of the true ozone value by a factor of two, as reported by *Mayer et al.* [1998], is unlikely for Barrow, as clouds with a cloud optical depth of more than 1000 as in the case analyzed by *Mayer et al.* [1998] were not observed at Barrow.

[33] Average reductions of erythemal UV are less than 5% in March and April. This low value is caused by fewer and thinner clouds during spring and the compensation of cloud attenuation by multiple reflections between cloud ceiling and high-albedo ground. The maximum cloud optical depth during these months is less than 25. Our calculations further indicate that the multiple reflections lead to an amplification of absorption of ozone molecules that are located between ground and cloud. For example, for a cloud with optical thickness of 15, which is located between 2 and 4 km over
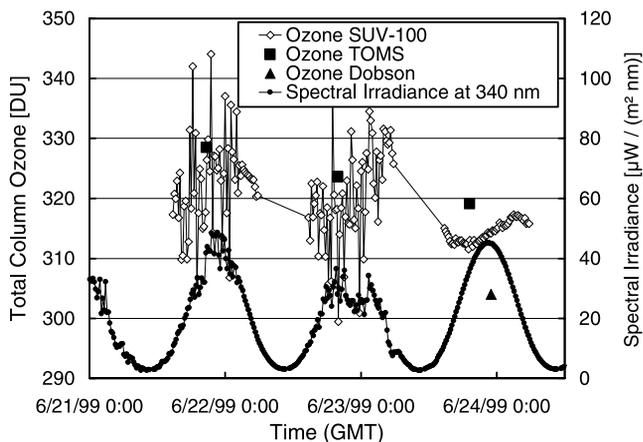
Figure 8. Effect of clouds on ozone retrieval.

snow-covered ground, ozone values are overestimated by 2% compared to 1% for snow-free ground.

[34] The second uncertainty related to clouds is caused by the fact that the SUV-100 is a scanning spectroradiometer. Measurements in the 300–315 and 325–335 nm ranges are about 1.5 min apart. During this time, radiation levels can significantly change, affecting the ratio R. The uncertainty was quantified by calculating ozone during cloudy days, and analyzing the dispersion in the result. Figure 8 shows ozone values for three consecutive days. The first day was cloudy in the morning and clear in the afternoon; the second day was overcast, and the third day was cloudless. TOMS measurements indicated that total ozone column during this period was constant to within 10 DU. SUV-100 ozone values vary smoothly with time on the third day but scatter considerably during the second day. For SZA < 75°, the standard deviation is 2.5% of the average. The first day indicates that there is no obvious step-change when the sky became clear around 2:30 UT. The standard uncertainty for the months June–October was consequently set to 2.5%. As cloudy days are less frequent in spring, the uncertainty for March and April was reduced to 1%.

4.4. Albedo

[35] Changing albedo from 0.85 to 0 in the model leads to 1.7% higher ozone values (Figure 9). The calculations are based on a clear-sky solar spectrum that was recorded at Barrow on April 28, 2001 with SZA = 59°. At Barrow, there is a pronounced cycle in albedo due to variations in snow cover and sea ice extent. Albedo leads to a wavelength-dependent increase in surface UV, with larger changes at shorter wavelengths [e.g., *Gröbner et al.*, 2000]. By comparing measured and modeled spectra at wavelengths that are not affected by ozone it was estimated that the effective albedo during winter in Barrow is 0.85 ± 0.1. The albedo during summer was assumed to be 0.05 ± 0.02, which is a typical range for water and pasture [*Blumthaler and Ambach*, 1988]. Measurements of local albedo in the visible performed at the CMDL station in Barrow suggest that albedo rapidly declines during snowmelt in late May and early June [*Dutton and Endres*, 1991], and increases again in October at the start of the winter.

[36] All ozone values discussed in the Results Section were calculated with a year-independent annual cycle in albedo, applying an albedo of 0.85 in months with snow cover, 0.05 in months without snow cover, and transition periods in June and October. Standard uncertainties were calculated to be 0.2% for winter, 0.02% for summer and 0.5% in June and October.

4.5. Aerosols and Ground Pressure

[37] According to *Climate Monitoring and Diagnostics Laboratory* (*CMDL*) [2002], the aerosol optical depth at 500 nm, τ, Ångstroem α, and single scattering albedo ω vary at Barrow between [$\tau = 0.05$, $\alpha = 1.8$, $\omega = 0.99$] (background conditions) and [$\tau = 0.25$, $\alpha = 0.4$, $\omega = 0.85$] (dust events). Resulting ozone uncertainties were estimated in a similar way as for albedo. Ground pressure was estimated to vary between 992 and 1038 hPa according to data from the National Climatic Data Center (NCDC).

4.6. Instrument-Related Uncertainties

[38] Uncertainties in the retrieved ozone values due to errors in the measured spectra mostly arise from wavelength errors in the instrument and uncertainty in the absolute calibration. Ozone calculated from a spectrum that was deliberately shifted by 0.1 nm deviated by 1.3% from the result calculated from the unshifted spectrum. The wavelength accuracy of published UV spectra is tested with an algorithm that compares the Fraunhofer structure in measured spectra with the same structure in a reference spectrum [*Slaper et al.*, 1995; *Booth et al.*, 2001]. The wavelength calibration uncertainty was found to be ±0.04 nm (±1σ), which translates into a 0.54% standard uncertainty in ozone.

[39] Wavelength-dependent errors in the instrument's absolute calibration also lead to errors in ozone. Based on the analysis of the instrument's calibration record (see NSF Network Operations Reports [e.g., *Booth et al.*, 2001]), we estimated that the maximum relative calibration error between the 300–315 nm and 325–335 nm wavelength bands is ±1.5%. We calculated further that a 5% error in ozone would require a 12.8% relative calibration error. From these numbers, we estimated the standard uncertainty in ozone to be 0.33%.
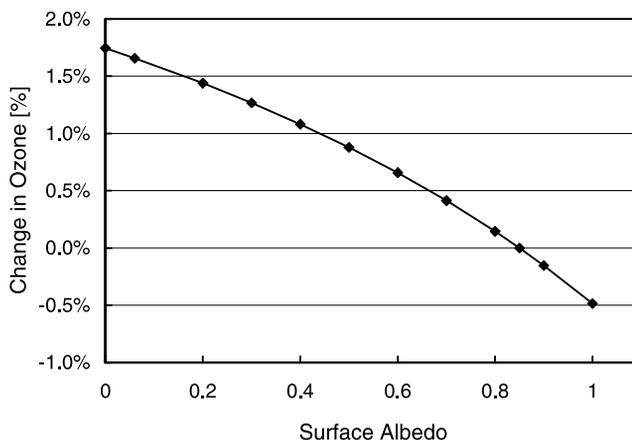

Figure 9. Sensitivity of ozone retrieval algorithm to changes in albedo. Data are normalized to albedo = 0.85.
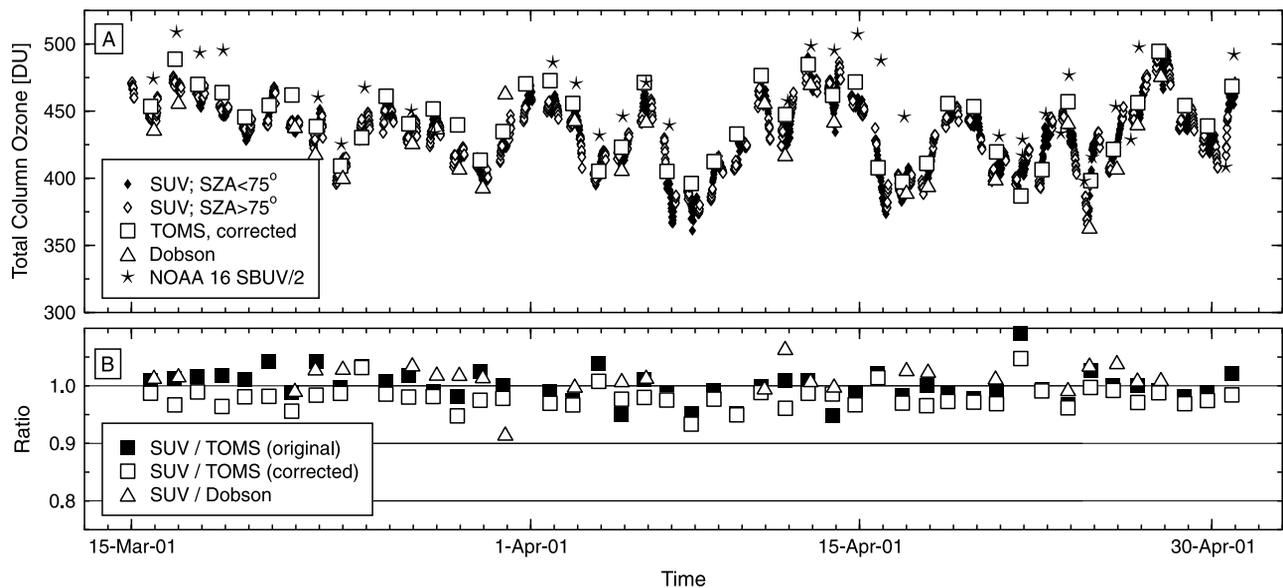
Figure 10. Comparison of ozone values calculated from the SUV-100 global irradiance spectra with TOMS, Dobson, and NOAA16 SBUV/2 observations during March and April 2001. (a) Total column ozone values from all data sets. (b) Ratio of SUV-100 data with TOMS and Dobson measurements. The ratios are based on SUV-100 spectra that were measured within ±15 min of TOMS and ±30 min of Dobson observations.

[40] The deviation of the SUV's angular response from the ideal cosine response is −5% at 60° and −10% at 70°. The error in measuring isotropic irradiance is −5% [*Bernhard et al.*, 2003]. Correction factors to compensate for these cosine errors are applied and range between 4.2% and 5.6% for wavelengths below 330 nm, depending on SZA. The effect of the cosine error on ozone retrievals is negligible as correction factors for the 300−315 nm and 325−335 nm wavelength bands differ by less than 0.2%, and this uncertainty is further reduced by the correction.

[41] As no detectable solar radiation can be expected below 290 nm, we subtract the average of the signal measured between 280 and 290 nm from the signal of the remaining solar scan [*Booth et al.*, 2001]. This subtraction removes the photomultiplier's dark current and most of the signal from stray light, should it exist. We estimate that the remaining contribution of stray light is below 0.001 mW/(m²nm). The contribution of stray light to the uncertainty budget is negligible since the ozone retrieval algorithm only uses wavelengths where the irradiance is larger than 1 mW/(m²nm). Uncertainties related to the instrument's finite bandwidth were found to be insignificant as well.

4.7. Radiative Transfer Model Related Uncertainties

[42] Finally, there may also be systematic errors caused by approximations applied within the radiative transfer model. For example, the sphericity of the Earth is not treated in an exact way, and this may lead to noticeable systematic errors when the sun in low. These errors are difficult to quantify and were therefore not included in the uncertainty budget. However, if the model input parameters are well-characterized, as they are for example at the South Pole, ratios of measured and modeled spectra for SZA = 84° show no significant wavelength dependence in the wave-length range relevant for the retrieval algorithm [*Bernhard et al.*, 2002]. It can therefore be assumed that model-related uncertainties are small.

5. Results
5.1. Comparison of SUV-100, TOMS, and Dobson Measurements During March and April 2001

[43] Figure 10 shows the comparison of column ozone values calculated from SUV-100 spectra with TOMS over-pass data and Dobson measurements at Barrow during March 15−April 30, 2001, the period of the TOMS³F campaign. Total column values from NOAA 16 profiles measured within ±1° latitude and ±5° longitude of Barrow are depicted as well. These values are higher than data from all other data sets.

[44] The SUV-100 data set was calculated with the TOMS16SW profiles. A temperature correction was applied based on stratospheric temperatures extracted from the CMDL profiles and using equation (2). Corrections vary between +0.3% in March and −0.8% at the end of April. Both the TOMS data set with and without scan mirror correction are presented. Figure 10a shows the variation of ozone measurements with time, and Figure 10b shows the ratios SUV/TOMS and SUV/Dobson. For the latter plot, only SUV-100 spectra measured within ±15 min of TOMS and ±30 min of Dobson observations were selected. SUV-100 data are in average 1.5 ± 2.6% higher than Dobson observations and 2.1 ± 2.0% lower than the scan-mirror corrected TOMS measurements. The bias between corrected TOMS and SUV-100 data is consistent with the average differences of 1.4 ± 2.4% observed for March and April during the years 1997−2000 (see below). Uncorrected TOMS data show no bias to SUV-100 data (SUV/TOMS = 0 ± 2.7%). Note that the standard deviation SUV/TOMS is

lower for the corrected data set. Further analysis did not indicate any significant dependence of the ratios on SZA.

[45] In Figure 10a the SUV-100 data set is split into measurements below and above 75° SZA. Measurements with SZA < 75° are only slightly affected by profile related uncertainties. They therefore allow the tracking of real changes in the atmospheric ozone amount during the course of a day. For example, ozone drops from 425 DU to 379 DU between 4/15/01 17:00 UT and 4/16/01 02:30 UT. The scatter introduced by clouds is generally smaller than the difference of TOMS and Dobson measurements as well as the observed diurnal changes in ozone. This demonstrates that SUV-100 measurements are suitable for monitoring short-term ozone variations.

5.2. Comparison of SUV-100, TOMS, and Dobson Measurements Between 1996 and 2001

[46] In order to evaluate the long-term performance of SUV-100 data, ozone values were calculated from SUV-100 spectra measured between 1996 and 2001 at times coinciding with TOMS and Dobson observations. As CMDL profile measurements at Fairbanks are too sparse to establish a climatology, and NOAA16 profiles were not available for the entire year, the set of semimonthly averaged NOAA 11 SBUV/2 profiles was used for ozone retrievals. Temperature corrections were based on CMDL profiles. Corrections vary between +0.2% in March and −2.6% in July.

[47] SUV-100 measurements are in average 2.2 ± 3.1% lower than TOMS measurements for the months February−June (Figure 11a). There is little dependence on SZA, even at SZA = 85°. This is somewhat fortuitous. For example, if the calculations had been carried out with the NOAA16 rather than NOAA11 profiles, ozone values for March 2001 would have been higher by about 3% at SZA = 80°. Ratios are generally lowest in May. During this month, the winter model albedo value of 0.85 was still used, and this value may have been too large if snowmelt occurred earlier. Part of the discrepancy could also be explained by a possible difference of prevailing stratospheric temperatures at Barrow, and the mean temperature of the CMDL profiles for May, which is 231 K.

[48] The scatter of the SUV/TOMS ratio can be reduced if measurements affected by changing cloud cover are filtered out. The black squares in Figure 11a are data that satisfy the conditions $|Q(340)/Q(350) -1|<1$ % and $|Q(330)/Q(360) -1| < 4$ %. For the filtered data set, the SUV/TOMS difference is −1.9 ± 2.2%. (Note that the standard deviation is considerably lower than for the unfiltered data set.) Clouds have a larger influence in the second half of the year (Figure 11b). For the July−October period, the SUV-100 data is lower than TOMS by 0.9 ± 3.7% for the unfiltered and 0.3 ± 2.4% for the filtered data set.

[49] The ratio SUV/Dobson is generally larger than SUV/TOMS, but also shows a slight dip in May (thin line Figure 11a). On the average, SUV measurements are higher than Dobson measurements by 1.8 ± 2.5% in spring and 0.9 ± 1.8% in fall (unfiltered data).

[50] For assessing possible drifts in the data sets of all three instruments, the daily ratios SUV/TOMS and SUV/Dobson were averaged over 14-day periods. Figure 12 shows the time-series of these semimonthly averages for
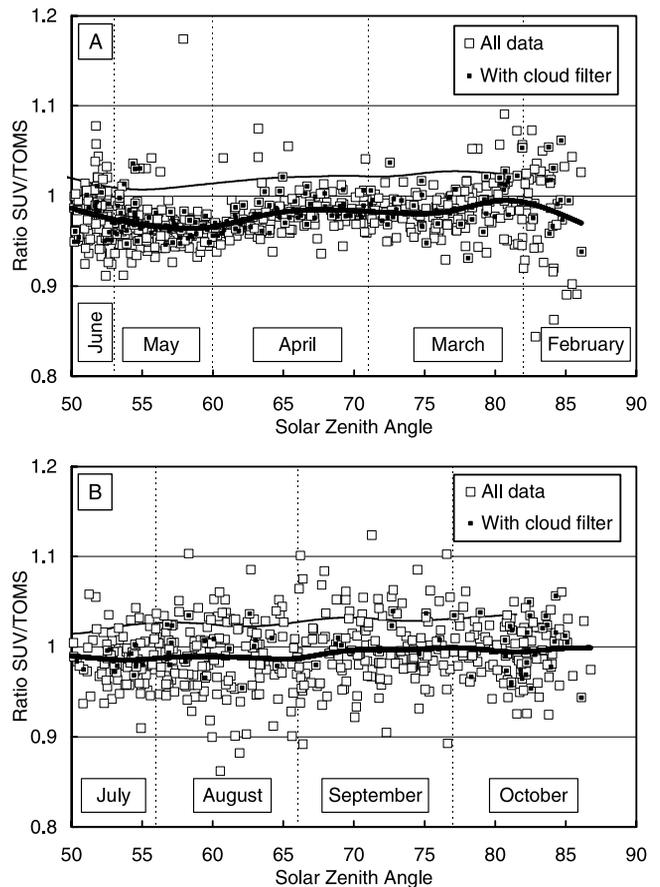

Figure 11. (a) Ratio of SUV to TOMS total column ozone values. SUV data were calculated with the semimonthly average NOAA 11 SBUV/2 profiles. Open squares show all data for the months February−June during the period 1996−2001. Black squares show a subset of the data filtered for cloud influence. The thick line is a fit line to the data. The thin line is the same fit for the ratio SUV/Dobson. (b) Same as Figure 11a for the months July−October.

the period July 1996 − June 2001. The standard deviation of the mean was calculated for every 14-day period from the random errors in Table 1, combined in quadrature with the systematic errors, and multiplied with a coverage factor of two. Thus, the error bars in Figure 12 give the 2-σ uncertainty of the semimonthly mean values. Uncertainties of TOMS and Dobson are not included.

[51] For most months, SUV-100 ozone values agree within the error bars with TOMS and Dobson measurements. With few exceptions, SUV-100 data are generally lower than TOMS and higher than Dobson measurements. A regression analysis confirmed that there is no significant drift between all three data sets at the 2-σ level. Both the corrected TOMS data from 2001 (black diamonds in Figure 12c) and the uncorrected data (open circles) agree within the scatter of years prior to 2001. The only exception is the uncorrected value for the second half of February 2001, which leads to the highest ratio (SUV/TOMS = 1.05) of the whole data set. The high value at the end of the year 2000 data series in Figure 12d (SUV/Dobson = 1.07) is the only point representing the 1−15 October period. The
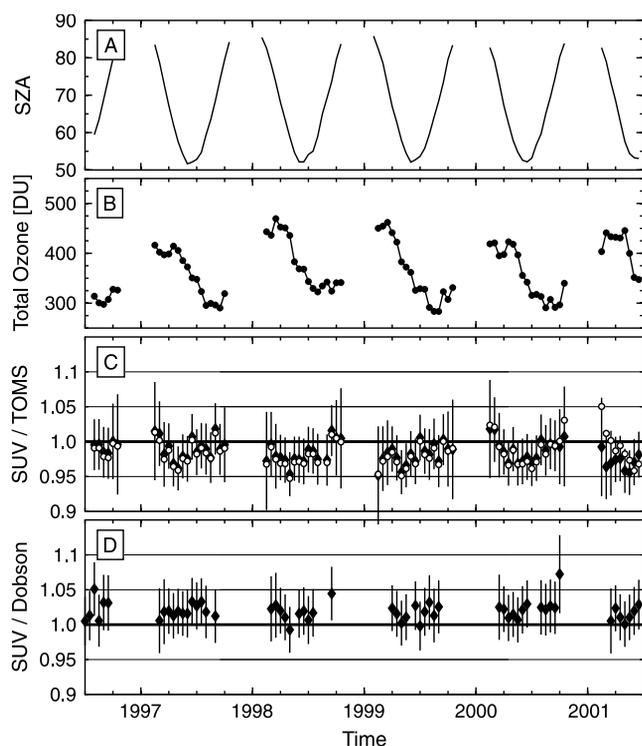
Figure 12. Comparison of semimonthly averages of SUV-100, TOMS, and Dobson ozone measurements at Barrow, observed during the years 1996–2001. (a) Average solar zenith angle of the included observations. (b) Semimonthly average total column ozone measured by SUV-100. (c) Ratio of semimonthly total ozone values measured by SUV-100 and TOMS. Scan-mirror corrected TOMS ratios are shown as black diamonds, uncorrected data as open circles. (d) Ratio of semimonthly total ozone values measured by SUV-100 and Dobson.

average SZA for this period is 84°, which is about the SZA up to which the algorithm can be trusted.

6. Discussion and Conclusions

[52] A new algorithm for the retrieval of total column ozone values from global irradiance spectra that has recently been developed was systematically checked for its accuracy and applied to measurements of the NSF/OPP SUV-100 spectroradiometer at Barrow, Alaska. The expanded (coverage factor 2) combined standard uncertainty of all systematic error sources was calculated and varies between 2 and 3.5% for SZA smaller than 75° and clear skies (see Table 1). These results are comparable with typical uncertainties of the TOMS and Dobson instruments [*Basher*, 1982; *McPeters and Labow*, 1996].

[53] For SZAs larger than 75°, the uncertainty budget of SUV-100 ozone retrievals becomes dominated by the sensitivity of the method to the ozone profile. For example, the expanded uncertainty from all systematic errors is 7% at SZA = 85°, if profiles are taken from a climatological average. The uncertainty can be reduced if actual profiles are available.

[54] This study demonstrates that the sensitivity to the profile at large SZAs is likely not a specific problem of the algorithm, but rather a principle limitation in the accuracy of any method used to calculate total ozone column from global irradiance spectra at large SZA. In principle, it should be possible to estimate ozone profiles from global irradiance spectra with a modified Umkehr algorithm. These profiles could then be used as input for the column retrieval, thus improving its accuracy. Whether or not this is feasible has yet to be shown. Clearly, this method cannot work if the sun does not set during summer at high latitudes.

[55] A second important source of uncertainty is the scatter introduced by clouds. As we have demonstrated, this scatter can be significantly reduced with simple filter algorithms. To further reduce cloud related uncertainties, ozone values could be calculated from diffuse rather than global irradiance model values whenever the direct beam of the sun is blocked. *Mayer and Seckmeyer* [1998] have shown that this approach indeed leads to a reduction of errors when the disk of the Sun is obstructed by mountains or optically thin clouds.

[56] Ozone values derived with the new method were compared with TOMS overpass data for Barrow and Dobson measurements performed at the Barrow CMDL station. SUV-100 measurements in spring are in average 2.2% lower than TOMS and 1.8% higher than Dobson measurements. There were no statistically significant drifts found in either the SUV-100, TOMS, or Dobson data sets. A difference of 4% between TOMS and Dobson at high latitudes is not unusual. A preliminary conclusion of the TOMS[3]F comparison was that much of the total ozone dependent difference between TOMS and Dobson was actually caused by internal scattering errors in the Dobson instrument used in this campaign. A systematic comparison of Nimbus 7 TOMS and the worldwide Dobson network reported by *McPeters and Labow* [1996] showed maximum deviations in the order of ±4%. Moreover, discrepancies between Dobson and Nimbus 7 TOMS measurements strongly increase for SZA above 80°; station-to-station differences at SZA = 85° may exceed 15%. *Wellemeyer et al.* [1997] have investigated the error in TOMS ozone values related to the uncertainty of the ozone profile in more detail. They found that at solar zenith angles greater than 80° the error due to profile shape uncertainty becomes significant. A reduction of this uncertainty required a modification of the TOMS algorithm that considers both mixing of profiles and use of the other TOMS wavelengths, but the error cannot be eliminated. This demonstrates that satellite ozone measurements at very large SZA are subject to very similar errors to ozone retrievals from global irradiance spectra measured at the ground.

[57] Based on our results we conclude that total column ozone for SZA smaller than 75° can be derived from global irradiance measurements with similar accuracy than that applicable to TOMS and Dobson observations. The SUV-100 data set can therefore be used for validating data from other sources. An additional benefit of global irradiance data is that they are typically available at high frequency, which supports the study of short-term variations in ozone or the interpolation of TOMS measurements to coincide with Dobson observations.

References

Anderson, G. P., S. A. Clough, F. X. Kneizys, J. H. Chetwynd, and E. O. Shettle, AFGL atmospheric constituents profiles (0–120 km), *Tech. Rep. AFGL-TR-86-0110*, Air Force Geophys. Lab., Sudbury, Mass., 1986.

Basher, R. E., Review of the Dobson Spectrophotometer and its accuracy, *WMO Rep. 13*, WMO Global Ozone Res. and Monit. Proj., Geneva, 1982.

Bass, A., and R. J. Paur, The ultraviolet cross sections of ozone: 1, The measurement, in *Atmospheric Ozone*, edited by C. Zerefos and A. Ghazi, pp. 606–616, D. Reidel, Norwell, Mass., 1985.

Bernhard, G., C. R. Booth, and J. C. Ehramjian, Comparison of measured and modeled spectral ultraviolet irradiance at Antarctic stations used to determine biases in total ozone data from various sources, in *Ultraviolet Ground- and Space-Based Measurements, Models, and Effects*, edited by J. R. Slusser, J. R. Herman, and W. Gao, *Proc. SPIE Int. Soc. Opt. Eng.*, *4482*, 115–126, 2002. (Also available at www.biospherical.com/nsf/presentations.asp)

Bernhard, G., C. R. Booth, and J. C. Ehramjian, The quality of data from the National Science Foundation's UV Monitoring Network for Polar Regions, in *Ultraviolet Ground- and Space-Based Measurements, Models, and Effects II*, edited by J. R. Slusser, J. R. Herman, and W. Gao, *Proc. SPIE Int. Soc. Opt. Eng.*, *4896*, 79–93, 2003. (Also available at www.biospherical.com/nsf/presentations.asp)

Blumthaler, M., and W. Ambach, Solar UVB-albedo of various surfaces, *Photochem. Photobiol.*, *48*(1), 85–88, 1988.

Booth, C. R., T. B. Lucas, J. H. Morrow, C. S. Weiler, and P. A. Penhale, The United States National Science Foundation's polar network for monitoring ultraviolet radiation, in *Ultraviolet Radiation in Antarctica: Measurements and Biological Effects*, *Antarct. Res. Ser.*, vol. 62, edited by C. S. Weiler and P. A. Penhale, pp. 17–37, AGU, Washington, D.C., 1994.

Booth, C. R., G. Bernhard, J. C. Ehramjian, V. V. Quang, and S. A. Lynch, NSF Polar Programs UV Spectroradiometer Network 1999–2000 operations report, Biospherical Instrum. Inc., San Diego, Calif., 2001. (Available at www.biospherical.com)

Brühl, C. H., and P. J. Crutzen, On the disproportionate role of tropospheric ozone as a filter against solar UV-B radiation, *Geophys. Res. Lett.*, *16*(7), 703–706, 1989.

Climate Monitoring and Diagnostics Laboratory (CMDL), Summary report, edited by D. B. King et al., *Rep. 26 2000–2001*, U.S. Dep. of Commer., Boulder, Colo., 2002.

Dutton, E. G., and D. J. Endres, Date of snowmelt at Barrow, Alaska, *Arct. Alp. Res.*, *23*(1), 115–119, 1991.

Götz, F. W. P., Zum Strahlungsklima des Spitzbergensommers, Strahlungs- und Ozonmessungen in der Königsbucht 1929, *31*, *Gerlands Beitr*, 119–154, 1931.

Gröbner, J., et al., Variability of spectral solar ultraviolet irradiance in an Alpine environment, *J. Geophys. Res.*, *105*(D22), 26,991–27,003, 2000.

International Standards Organization (ISO), Guide to the expression of uncertainty in measurement, Geneva, 1993.

Masserot, D., J. Lenoble, C. Brogniez, M. Houet, N. Krotkov, and R. McPeters, Retrieval of ozone column from global irradiance measurements and comparison with TOMS data: A year of data in the Alps, *Geophys. Res. Lett.*, *29*(9), 23, 2002.

Mayer, B., and G. Seckmeyer, Retrieving ozone columns from spectral direct and global UV irradiance measurements, in *Proceedings of XVIII Quadrennial Ozone Symposium-96, September 12–21, 1996*, edited by R. D. Bojkov and G. Visconti, pp. 935–938, Edigrafital S.P.A. - S. Atto (TE), 1998.

Mayer, B., A. Kylling, S. Madronich, and G. Seckmeyer, Enhanced absorption of UV radiation due to multiple scattering in clouds: Experimental evidence and theoretical explanation, *J. Geophys. Res.*, *103*(D23), 31,241–31,254, 1998.

McPeters, R. D., and G. J. Labow, An assessment of the accuracy of 14.5 years of Nimbus 7 TOMS Version 7 ozone data by comparison with the Dobson network, *Geophys. Res. Lett.*, *23*(25), 3695–3698, 1996.

McPeters, R. D., G. J. Labow, and B. J. Johnson, A satellite-derived ozone climatology for balloonsonde estimation of total column ozone, *J. Geophys. Res.*, *102*(D7), 8875–8885, 1997.

Seckmeyer, G., and G. Bernhard, Cosine error correction of spectral UV irradiances, in *Atmospheric Radiation*, *Proc. SPIE Int. Soc. Opt. Eng.*, *2049*, 140–151, 1993.

Slaper, H., H. A. J. M. Reinen, M. Blumthaler, M. Huber, and F. Kuik, Comparing ground level spectrally resolved solar UV measurements using various instruments: A technique resolving effects of wavelength shift and slit width, *Geophys. Res. Lett.*, *22*(20), 2721–2724, 1995.

Stamnes, K., J. Slusser, and M. Bowen, Derivation of total ozone abundance and cloud effects from spectral irradiance measurements, *Appl. Opt.*, *30*(30), 4418–4426, 1991.

Wellemeyer, C. G., S. L. Taylor, C. J. Seftor, R. D. McPeters, and P. K. Bhartia, A correction for total ozone mapping spectrometer profile shape errors at high latitude, *J. Geophys. Res.*, *102*(D7), 9029–9038, 1997.

———————————

G. Bernhard and C. R. Booth, Biospherical Instruments Inc., 5340 Riley Street, San Diego, CA 92110, USA. (bernhard@biospherical.com)

R. D. McPeters, NASA Goddard Space Flight Center, Greenbelt, MD 20771, USA.